The Scaling of Human Interactions with City Size

Markus Schläpfer[1]*, Luís M. A. Bettencourt[2], Mathias Raschke[3], Rob Claxton[4], Zbigniew Smoreda[5], Geoffrey B. West[2], Carlo Ratti[1]

[1]Senseable City Laboratory, Massachusetts Institute of Technology, Cambridge, Massachusetts, USA.
[2]Santa Fe Institute, 1399 Hyde Park Rd, Santa Fe, New Mexico 87501, USA.
[3]Mathias Raschke, Leipzig, Germany.
[4]British Telecommunications plc, Ipswich, UK.
[5]Orange Labs, Issy-les-Moulineaux, France.
*Correspondence to: schlmark@mit.edu.

The pace of life accelerates with city size, manifested in a per capita increase of almost all socioeconomic rates such as GDP, wages, violent crime or the transmission of certain contagious diseases. Here, we show that the structure and dynamics of the underlying network of human interactions provides a possible unifying mechanism for the origin of these pervasive regularities. By analyzing billions of anonymized call records from two European countries we find that human social interactions follow a superlinear scale-invariant relationship with city population size. This systematic acceleration of the interaction intensity takes place within specific constraints of social grouping. Together, these results provide a general microscopic basis for a deeper understanding of cities as co-located social networks in space and time, and of the emergent urban socioeconomic processes that characterize complex human societies.

The pace of life systematically accelerates with city size - literally, people tend to walk faster in larger cities (*1*). Similar increases apply to a wide spectrum of socioeconomic quantities, including GDP, wages, patents, violent crime and certain contagious diseases (*2-5*). With rare exception, these aggregated urban quantities, Y, are well described, on average, by superlinear scale-invariant relationships with city population size, N, $Y \propto N^\beta$ with a common exponent $\beta \approx 1.15 > 1$ (*6, 7*). It has been proposed that these scaling relations are rooted in a universal structure and dynamics of the underlying network of human social interactions common to all cities (*6, 8, 9*). However, this hypothesis has never been tested, largely due to limitations in the availability of extensive data covering the population of entire urban systems. The vast majority of previous studies on detailed human interactions in cities has relied on survey-based approaches, which are constrained by small sample sizes and few places surveyed, and are biased towards strong social links (*10, 11*).

In order to fill this gap, we analyzed networks of human interactions inferred from large datasets of anonymized mobile phone and landline telecommunication records in two European countries. In these networks, each person is modeled as a node, connected to others by links, weighted by their communication intensity. In order to characterize the variation of human social interactions with city size, we examined (i) the number of links per person ('degree'), (ii) the communication time and number of calls ('link intensity') and (iii) the probability that one person's contacts are also connected to each other ('clustering'). These three quantities are key to defining network models of social interactions, such as disease transmission or information diffusion: the degree and link intensity tell us how fast the state of a node may spread to nearby nodes (*12-15*), while the clustering largely determines its probability of propagating beyond the initial node's immediate neighbors (*16, 17*).

2

The first dataset analyzed contains 440 million mobile phone call records collected in Portugal during 15 months, covering approximately 20% of the country's population. The resulting interaction network has 1.6×10^6 nodes and 6.8×10^6 links (reciprocated social ties). We mapped users to cities based on the location of their most frequently used cell tower (*18*). The second dataset contains 7.6×10^9 landline call records collected in the UK over a month and covers more than 90% of the national landline numbers as well as their connections to mobile phones. The resulting network has 47×10^6 nodes and 119×10^6 reciprocated links. The assignment of nodes to cities in the UK is based on regional telephone exchange areas (*18*).

Figure 1A depicts the cumulative degree $K = \sum_{i \in S} k_i$ for each city in Portugal (140 Statistical Cities, 9 Larger Urban Zones and 293 Municipalities), versus its population size, N. Here, S is the set of nodes assigned to a given city and k_i denotes the degree of node i. At face value, the variance in $K(N)$ is large, even between cities of similar size, so that a mathematical relationship between K and N is difficult to characterize. However, most of this variation is likely due to the uneven distribution of the telecommunication provider's market share, which, for each city, can be estimated by the relative coverage $s = |S|/N$ (*18*). If the cumulative degree is rescaled by s, $K_r = K/s$, the resulting variance as a function of population size is significantly reduced (Fig. 1B). More importantly, the relationship between K_r and N is now well characterized by a simple power law with exponent $\beta = 1.12 > 1$. This superlinear scaling holds over several orders of magnitude and its exponent is in excellent agreement with that of most observed urban socioeconomic indicators and theoretical expectations (*6, 8*). It is worth emphasizing that the seemingly small excess of β above unity implies a substantial increase in the level of social interaction with city size: every doubling of a city's population results, on

3

average, in approximately 12% more mobile phone contacts per person. This implies that during the observation period (15 months) an average urban dweller in Lisbon (Statistical City, $N \approx 5 \times 10^5$) accumulated about twice as many reciprocated contacts as an average resident of Lixa, a rural town (Statistical City, $N \approx 4 \times 10^3$, see Fig. 1C). Superlinear scaling with similar values of the exponents also characterizes both the population dependence of the rescaled cumulative call volume, $V_r = \sum_{i \in S} v_i / s$, where v_i is the total time user i spent on the phone, and of the rescaled cumulative number of calls, $W_r = \sum_{i \in S} \omega_i / s$, where ω_i denotes the total number of calls initiated or received by user i (Table 1). Thus, the average number of links per user, $\langle k \rangle = K / |S|$, the average call volume per user, $\langle v \rangle = V / |S|$, and the average number of calls per user, $\langle \omega \rangle = W / |S|$, all scale in a similar fashion as $N^{\beta-1}$ with $\beta \approx 1.10$. Together, these results imply that, on average, both the total time spent on the phone and the number of calls per contact ($\langle v \rangle / \langle k \rangle$ and $\langle \omega \rangle / \langle k \rangle$, respectively) are invariant with city size.

Table 1 shows that the superlinear scaling of the three interaction indicators persists throughout all city definitions applied to Portugal, and for different observation periods. Interestingly, if we further include all non-reciprocated social ties into the network (resulting in 1.8×10^6 nodes and 11×10^6 links), the scaling exponent for the cumulative degree increases (e.g., $\beta = 1.24$ for Statistical Cities). This suggests that the number of transitory social interactions grows even faster with city size than reciprocated contacts. Extending our study to the UK landline data confirms these findings. Despite the relatively short observation period of 31 days, the scaling exponents for all interaction indicators are significantly larger than unity (Table 1). Superlinear scaling thus seems to hold across both different means of communication and different national urban systems.

4

Previous studies on urban scaling have been limited to aggregated, city-wide quantities (*6, 7*), mainly due to limitations in the availability and analysis of extensive individual-based data. Here, we leverage the granularity of our data to explore how the scaling relations emerge from the underlying distributions of network properties. We focus on Portugal's mobile phone network which, in contrast to landline connections, provides a more direct proxy for person-to-person interactions (*19, 20*). Moreover, we considered only regularly active callers who initiated and received at least one call during each successive period of 3 months, so as to avoid a potential bias towards longer periods of inactivity (Fig. S3). The statistical distributions of the nodal degree, call volume and number of calls are remarkably regular across diverse urban settings (Fig. 2). The distribution of the degree is well described by a skewed lognormal distribution (i.e., $k^* = \ln k$ follows a skew-normal distribution), while both the call volume and the number of calls are well approximated by a conventional lognormal distribution (i.e., $v^* = \ln v$ and $\omega^* = \ln \omega$ follow a Gaussian distribution). The mean values of all logarithmic variables are consistently increasing with city size, while the variances are approximately constant (Fig. 2, insets); this implies that superlinear scaling is not simply due to the dominant effect of a few individuals but to a set of multiplicative random processes that involve most people in the city. More generally, we should also note that lognormal distributions typically appear as the limit of many random multiplicative processes (*21*); this suggests that social ties are the result of generating new acquaintances through a cascade of stochastic sequences in space and time.

Finally, we examined the local clustering coefficient, C_i, which measures the fraction of connections between one's social contacts, relative to all possible connections between them

(22); that is $C_i \equiv 2z_i / \left[k_i (k_i - 1) \right]$, where z_i is the total number of links between the k_i

neighbours of node i. A high value of C_i (close to unity) indicates that all of one's contacts also

know each other, while for $C_i = 0$ they are mutual strangers. As larger cities provide a larger

pool from which to select contacts, the probability that two contacts are also mutually connected

should decrease if they were established at random. Most measured and modeled human

networks also show a decrease of the clustering coefficient with increasing degree (23).

However, we find that the average clustering coefficient, $\langle C \rangle = \sum_{i \in S} C_i / |S|$, is an invariant of

city size and takes a value of 0.25 in Portugal (Fig. 3). We can understand both its invariance and

value by considering how the network grows as people are added to the city. The scaling relation

implies that with each new person the number of links in the network increases by $\Delta K = \beta \langle k \rangle$,

assuming that $K \propto N^\beta$ holds for $s = 1$. If the new person creates k_0 new attachments, then in

order to preserve the same clustering, its neighbors need to create new connections between

them, and their neighbors need to do the same, and so on, leading to structural changes

throughout the network. Details of such a process, constrained by keeping a constant clustering

coefficient, are given in (18). A simple consistency argument can be invoked to estimate the

leading order effect: on average, $\langle k \rangle$ new links are added with each new node and, if the

clustering coefficient is to be kept fixed, these induce $\sim \langle z \rangle / \langle k \rangle$ additional 'second order' links

between the neighbors of these new nodes. Thus, when ΔN new 'average' users join the

network, the total number of new links is approximately given by $\Delta K \sim \left[\langle k \rangle + \langle z \rangle / \langle k \rangle \right] \Delta N$. In

terms of an average clustering coefficient, $\langle C \rangle$, this can be expressed as

$\Delta K / \Delta N \sim \langle k \rangle + \langle C \rangle (\langle k \rangle - 1) / 2$, leading to $\beta \approx 1 + \langle C \rangle (\langle k \rangle - 1) / 2 \langle k \rangle \approx 1 + \langle C \rangle / 2$, or

6

$\langle C \rangle \approx 2(\beta - 1)$. With $\beta \approx 1.12$, this gives $\langle C \rangle \approx 0.24$ in excellent agreement with the data. Taking the calculation to higher orders (*18*) yields the upper bound $\beta < 1 + \langle C \rangle / \left[2(1 - 2\langle C \rangle) \right] \approx 1.25$.

These results show that as cities grow, human interactions accelerate within well-defined behavioral constraints. Moreover, the invariance of the clustering coefficient expresses another important aspect of urban life: even in large cities we live in groups that are as tightly knit as those in small towns or 'villages' (*24*). However, in a real village we may need to accept a community imposed on us by sheer proximity, whereas in a city we can 'choose' our own village - a community of people with shared interests, background, profession, ethnicity, sexual orientation, etc. - with more intense and dynamic interactions, evolving over time.

To our knowledge, the results presented here constitute the first extensive empirical evidence of the acceleration of human interactions in cities. Their superlinear scaling with city size shows an exponent in remarkably good agreement with those observed in almost all socioeconomic metrics, strongly suggesting that the 'universality' of the structure and dynamics of networks of human interactions underlies the generic properties of cities (*8*). In combination with other geographic and socioeconomic data (*25*) our findings may serve as a quantitative foundation for microscopic, interaction-based models of human societies across their many aspects, from economics (*2*) and sociology (*26, 27*) to urban planning (*28*) – possibly helping elucidate the mysterious forces that for many millennia now have impelled people to live in cities.

References and Notes:

1. S. Milgram, The experience of living in cities. *Science* **167**, 1461-1468 (1970).

2. M. Fujita, P. Krugman, A. J. Venables, *The Spatial Economy: Cities, Regions, and International Trade*. (MIT Press, Cambridge, MA, 2001).

3. L. Sveikauskas, The productivity of cities. *Q. J. Econ.* **89**, 393-413 (1975).

4. J. B. Cullen, S. D. Levitt, Crime, urban flight, and the consequences for cities. *Rev. Econ. Stat.* **81**, 159–169 (1999).

5. Centers for Disease Control and Prevention - HIV Surveillance in Urban and Nonurban Areas. Available at: <http://www.cdc.gov> (2012).

6. L. M. A. Bettencourt, J. Lobo, D. Helbing, C. Kühnert, G. B. West, Growth, innovation, scaling, and the pace of life in cities. *Proc. Natl Acad. Sci.* USA **104**, 7301-7306 (2007).

7. L. M. A. Bettencourt, G. B. West, A unified theory of urban living. *Nature* **467**, 912-913 (2010).

8. L. M. A. Bettencourt, The origins of scaling in cities. *Santa Fe Institute Working Paper #12-09-014* (Santa Fe Institute, Santa Fe, NM, 2012).

9. S. Arbesman, J. M. Kleinberg, S. H. Strogatz, Superlinear scaling for innovation in cities. *Phys. Rev. E* **79**, 016115 (2009).

10. C. S. Fisher, *To Dwell Among Friends: Personal Networks in Town and Country*. (Univ. Chicago Press, Chicago, 1982).

11. B. Wellman, *Networks in the Global Village: Life in Contemporary Communities*. (Westview Press, Boulder, CO, 1999).

12. E. M. Rogers, *Diffusion of Innovation* (Free Press, New York, 1995).

13. R. M. Anderson, R. M. May, *Infectious Diseases of Humans: Dynamics and Control* (Oxford Univ. Press, Oxford, 1991).

14. S. Eubank, Modelling disease outbreaks in realistic urban social networks. *Nature* **429**, 180–184 (2004).

15. R. Pastor-Satorras, A. Vespignani. Epidemic spreading in scale-free networks. *Phys. Rev. Lett.* **86**, 3200–3203 (2001).

16. M. E. J. Newman, Random graphs with clustering. *Phys. Rev. Lett.* **103**, 058701 (2009).

17. M. Granovetter, The strength of weak ties. *Am. J. Sociol.* **78**,1360-1380 (1973).

18. See supplementary materials.

19. J.-P. Onnela, et al. Structure and tie strength in mobile communication networks. *Proc. Natl. Acad. Sci. U.S.A.* **104**, 7332-7336 (2007).

20. M. C. González, C. A. Hidalgo, A.-L. Barabási, Understanding individual human mobility patterns. *Nature* **453**, 779–782 (2008).

21. M. Mitzenmacher, A brief history of generative models for power law and lognormal distributions. *Internet Math.* **1**, 226–251 (2004).

22. D. J. Watts, S. H. Strogatz, Collective dynamics of 'small-world' networks. *Nature* **393**, 440-442 (1998).

23. E. Ravasz, A.-L. Barabási, Hierarchical organization in complex networks. *Phys. Rev. E* **67**, 026112 (2003).

24. J. Jacobs, *The Death and Life of Great American Cities*. (Random House, New York, 1961).

25. N. Eagle, M. Macy, R. Claxton, Network diversity and economic development. *Science* **328**, 1029-1031 (2010).

26. S. Wasserman, K. Faust, *Social Network Analysis: Methods and Applications*. (Cambridge Univ. Press, New York, 1994).

27. D. Lazer et al., Computational social science. *Science* **323**, 721-723 (2009).

28. M. Batty, The size, scale, and shape of cities. *Science* **319**, 769-771 (2008).

Country	City definition	Entities	Caller network	ΔT	Y	β	95% CI
Portugal	Statistical City	140	reciprocal	409 days	Degree (K_r)	1.12	[1.11 1.14]
					Call volume (V_r)	1.11	[1.09 1.12]
					Number of calls (W_r)	1.10	[1.09 1.11]
				92 days	Degree (K_r)	1.10	[1.09 1.11]
					Call volume (V_r)	1.10	[1.08 1.11]
					Number of calls (W_r)	1.08	[1.07 1.10]
			non-reciprocal	409 days	Degree (K_r)	1.24	[1.22 1.25]
					Call volume (V_r)	1.14	[1.12 1.15]
					Number of calls (W_r)	1.13	[1.12 1.14]
	Larger Urban Zone	9(8)	reciprocal	409 days	Degree (K_r)	1.05	[1.00 1.11]
					Call volume (V_r)	1.11	[1.02 1.20]
					Number of calls (W_r)	1.10	[1.05 1.15]
			non-reciprocal	409 days	Degree (K_r)	1.13	[1.08 1.18]
					Call volume (V_r)	1.14	[1.05 1.23]
					Number of calls (W_r)	1.13	[1.08 1.18]
	Municipality	293	reciprocal	409 days	Degree (K_r)	1.13	[1.11 1.14]
					Call volume (V_r)	1.15	[1.13 1.17]
					Number of calls (W_r)	1.13	[1.11 1.14]
UK	Urban Audit City	24	reciprocal	31 days	Degree (K)	1.08	[1.05 1.12]
					Degree, land-mob (K^{lm})	1.14	[1.11 1.17]
					Call volume (V)	1.10	[1.07 1.14]
					Number of calls (W)	1.08	[1.05 1.11]

Table 1. Scaling exponents for different social interaction metrics and city definitions. The observation period of $\Delta T = 409$ days corresponds to the full extent of the dataset from Portugal, while $\Delta T = 92$ days is limited to the first three consecutive months. For the call volume statistics, we discarded 1 Larger Urban Zone (Ponta Delgada) due to a high estimation error of V_r (s.e.m. > 20%). For the UK data, the interaction indicators are not rescaled by the coverage, due to the high market share of the landline numbers. The dataset did not contain spatial information of the mobile phones. Thus, mobile phones are included only in terms of their reciprocated connections to landlines assigned to cities. The indicator K^{lm} denotes the cumulative number of links between landlines and mobile phones only (i.e., landline-landline connections are excluded). The exponents, β, are estimated using the nonlinear least squares method (trust-region method). For all values of β, Adj-R^2>0.98.
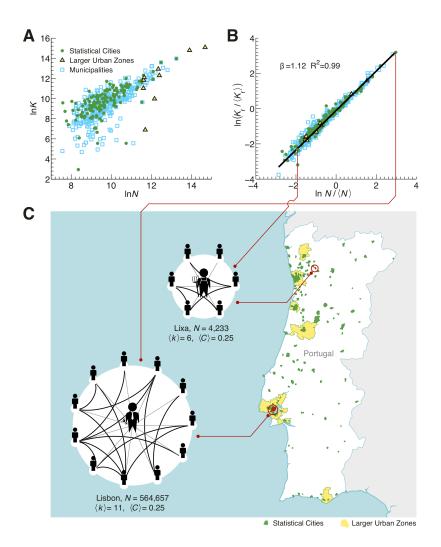
11

Fig. 1. Human social interactions scale superlinearly with city size. (**A**) Cumulative degree, K, versus city size in terms of population, N, for three different city definitions. (**B**) Collapse of K onto a single curve when rescaling based on relative coverage. For each city definition, the single values of K_r and N are normalized by their corresponding average values, $\langle K_r \rangle$ and $\langle N \rangle$, respectively, for direct comparability across different city definitions. (**C**) An average urban dweller of Lisbon has approximately twice as many reciprocated mobile phone contacts, $\langle k \rangle$, than an average individual in the rural town of Lixa. The fraction of mutually interconnected contacts (black lines) remains surprisingly unaffected, as indicated by the invariance of the average clustering coefficient, $\langle C \rangle$. The map further depicts the location of Statistical Cities and Larger Urban Zones, with the exception of those located on the archipelagos of the Azores and Madeira.
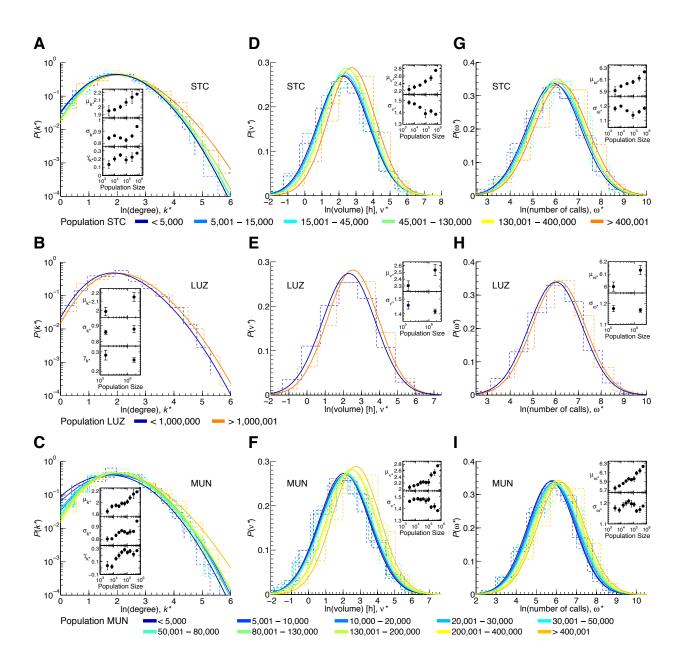
Fig. 2. The impact of city size on human interactions at the individual level. **(A)-(C),** Degree distributions, $P\left(k^{*}\right)$, for Statistical Cities (STC), Larger Urban Zones (LUZ) and Municipalities (MUN); the individual cities are log-binned according to their population size. The dashed lines indicate the underlying histograms and the continuous lines are best fits of the skew-normal distribution with mean $\mu_{k^{*}}$, standard deviation $\sigma_{k^{*}}$ and skewness $\gamma_{k^{*}}$ (insets). **(D)-(F),** Distributions of the call volume, $P\left(v^{*}\right)$ and, **(G)-(I),** number of calls, $P\left(\omega^{*}\right)$; the continuous lines are best fits of the normal distribution with mean values $\mu_{v^{*}}$ and $\mu_{\omega^{*}}$, and standard

13

deviations σ_{v*} and $\sigma_{\omega*}$, respectively (insets). The error bars correspond to the standard error of the mean (s.e.m.). The distribution parameters are estimated by the maximum likelihood method.
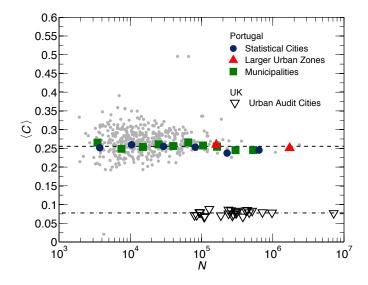
Fig. 3. The average clustering coefficient remains largely unaffected by city size. The dashed and dash-dotted lines correspond to the average values of all nodes in the networks of Portugal and UK, approximately 0.25 and 0.08, respectively. For Portugal, the individual cities are log-binned according to their population size to compensate for the varying market share of the telecommunication provider. The error bars (s.e.m.) are smaller than the symbols. Grey points are the underlying scatter plot for all cities. The value of $\langle C \rangle$ in the UK is lower than in Portugal, as expected for a landline network that captures the aggregated activity of different household members or business colleagues. If we were to assume that an average landline in the UK is used by 3 people who communicate with a separate set of unconnected acquaintances, we would indeed expect that the clustering coefficient measured at that landline would be approximately 1/3 of that of each individual.

Supplementary Materials for

The Scaling of Human Interactions with City Size

Markus Schläpfer,* Luís M. A. Bettencourt, Mathias Raschke, Rob Claxton, Zbigniew Smoreda, Geoffrey B. West, Carlo Ratti

*correspondence to: schlmark@mit.edu.

TABLE OF CONTENTS

PART 1. DATA

I . Urban population statistics and geospatial data

<u>Portugal</u>

Four different definitions of urban agglomerations were analyzed with respect to their social network scaling behavior: (i) Statistical Cities, (ii) Municipalities, (iii) Larger Urban Zones and (iv) Urban Audit Cities. The *Statistical Cities* (STC) and *Municipalities* (MUN) are defined by the national statistics office of Portugal ('Statistics Portugal') (*1*), which provided us with the population data according to the census 2001, and with the corresponding perimeters (shapefiles containing spatial polygons). The concepts of *Larger Urban Zones* (LUZ) and *Urban Audit Cities* (UAC) have been created by the European Union (EU) statistical agency ('Eurostat'), aimed at consistently comparing cities across different nations. The corresponding population statistics and shapefiles are publicly available (*2*). For the LUZ and UAC we compiled the population data for 2001 in order to assure direct comparability with the STC and MUN. In total, there are 156 STC, 308 MUN, 9 LUZ and 9 UAC. In contrast to all other agglomeration types, the MUN are an administrative subdivision of Portugal and thus partition the entire national territory. Although their interpretation as urban units is flawed in some cases, the MUN were included in the study as they cover the total resident population of Portugal and constitute the largest set of agglomeration entities. Furthermore, there are 6 entirely urban MUN, each of which corresponds to a STC. The UAC also follow administrative boundaries and therefore constitute a subset of the MUN. The LUZ correspond to functional urban regions, as they extend the UAC to their surrounding areas with substantial commutes into the cities (*2*).

<u>UK</u>

We focussed our study on the UAC as defined by Eurostat, and on the corresponding population statistics for 2001 (*2*). This allows for a direct comparison with the UAC (i.e., MUN) in Portugal. In total, the UK contains 30 UAC, which are equivalent to the European definition of Local Administrative Units, Level 1 (LAU-1, previously termed NUTS-4).

II. Telecommunication data

Portugal

The dataset analyzed in the main text consists of ≈ 440 million Call Detail Records (CDR) from the years 2006 and 2007, covering the voice call activity of ≈ 2 million mobile phone users and thus $\approx 20\%$ of the country's population (in 2006 the total mobile phone penetration rate was $\approx 100\%$ (*3*)). The data has been collected by a single telecom service provider for billing and operational purposes. The overall observation period is $\Delta T = 15$ months during which the data from 46 consecutive days is lacking, resulting in an effective analysis period of 409 days. To safeguard privacy, individual phone numbers were anonymized by the operator and replaced with a unique security ID. Each CDR consists of the IDs of the two connected individuals, the call duration, the date and time of the call initiation, as well as the unique IDs of the two cell towers routing the call at its initiation. In total, there are 6511 cell towers for which the geographic location was provided, each serving on average an area of ≈ 14 km^2, which reduces to ≈ 0.13km^2 in urban areas.

UK

The dataset contains ≈ 7.6 billion calls from a period of one month in 2005, involving ≈ 44 million landline numbers and ≈ 56 million mobile phone numbers. To retain customer anonymity and privacy, each phone number was replaced with a random, surrogate ID by the operator before providing the data. As these voice call records have been collected by a landline operator, we have only partial access to the connections made between any two mobile phones. The operator partitioned the country into ≈ 5500 exchange areas (covering 49 km^2 on average), each of which comprises a set of landline phone numbers. The dataset contains the geographic location of ≈ 4000 exchange areas (coordinates of the center points).

PART 2. SPATIAL INTERACTION NETWORKS

I. Portugal

Data filtering and resulting network characteristics

We inferred two distinct types of interaction networks from the CDRs: in the *reciprocal* (REC) network each node represents a mobile phone user and two nodes are connected by an undirected edge if each of the two corresponding users initiated at least

one call to the other. In the *non-reciprocal* (nREC) network two nodes are connected if there has been at least one call between them. The nREC network thus contains one-way calls which were never reciprocated, presumably representing more superficial interactions between individuals which might not know each other personally (*4*). Nevertheless, we eliminated all nodes which never received or never initiated any call, so as to avoid a potential bias induced by call centers and other business hubs. We performed our study on the largest connected cluster (LCC, giant component) extracted from both network types. Table S1 summarizes the basic network characteristics.

Network type	ΔT [days]	n	m	$\langle k \rangle$	$\langle v \rangle$ [hours]	$\langle \omega \rangle$	LCC
REC	409	1,589,511	6,770,405	8.52	18.03	498.56	0.98
	92	1,087,722	2,867,400	5.27	5.54	158.03	0.93
nREC	409	1,802,802	11,354,604	12.60	17.22	473.85	0.99

Table S1. Summary statistics for the mobile phone networks in Portugal. The size of the largest connected component (LCC) is given as a fraction of the total number of nodes. The values for the number of nodes n, number of links m, average degree $\langle k \rangle$, average call volume $\langle v \rangle$ and average number of calls $\langle \omega \rangle$ correspond to those of the LCC.

Assigning nodes to urban agglomerations

In order to assign a given mobile phone user to one of the different urban agglomerations, we first determined the cell tower which routed most of his calls. The area serviced by this 'characteristic' tower presumably represents his or her home place (*4*). Subsequently, the corresponding coordinate pairs were mapped to the polygons (shapefiles) of the different agglomerations. Following this assignment procedure, we were left with 140 STC (we discarded 5 STC for which no shapefile was available and 11 STC without any assigned cell tower), 9 LUZ and 293 MUN (we discarded 15 MUN without any assigned cell tower). Table S2 lists the statistics of the total resident population according to the census 2001. Figures S1A-C depict the size distribution of the analyzed agglomerations as traditional Zipf plots, where the logarithm of the rank is displayed versus the logarithm of the population size.

Agglomeration type	No. of entities	N^{tot}	N^{min}	N^{max}
Statistical Cities	140	4,032,176	1,960	564,657
Municipalities	293	9,901,216	1,924	564,657
Larger Urban Zones	9	4,566,630	108,891	2,363,470
Urban Audit Cities	9	1,555,558	58,051	564,657

Table S2. Population statistics of the analyzed urban agglomerations for the year 2001. For each city definition we show the total population covered, N^{tot}, as well as the population size of the smallest (N^{min}) and largest (N^{max}) entity.
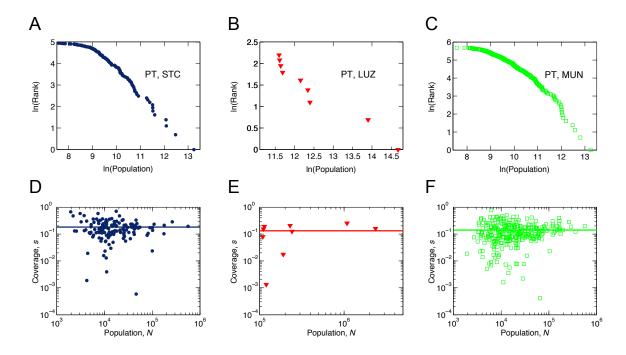

Fig. S1. Agglomeration population size distribution and relative number of assigned callers. **(A-C)** Zipf plots for Statistical Cities **(A)**, Larger Urban Zones **(B)** and Municipalities **(C)**. **(D-F)** Corresponding mobile phone coverage resulting from the node assignment procedure (REC network with ΔT =409 days). The solid lines show the average values.

The number of nodes assigned to each agglomeration, $|S|$, is strongly correlated with the corresponding population size, N (r =0.95 for STC, r =0.97 for LUZ and

$r=0.92$ for MUN), validating the assumed relation between the characteristic cell tower and the home location. Figures S1D-F show the coverage $s=|S|/N$ for each agglomeration with average values of $\langle s \rangle =0.18, 0.13, 0.14$ for STC, LUZ and MUN, respectively. We find negligibly small correlations between the coverage and the population size ($r=-0.02$ for STC and $r=0.09$ for MUN) except for the 9 LUZ ($r=0.34$) where the correlation is mainly induced by a very low coverage of two smaller entities located on the Azores and the island of Madeira. The otherwise low correlation levels strongly indicate that there is no asymmetric distribution of subscribers with respect to the population size of the agglomerations. Alternative node assignment methods may be equally applicable. To verify our results, we additionally determined the characteristic cell tower by considering only those calls which were initiated between 10pm and 7am, yielding qualitatively similar findings to those reported in the main text.

II. UK

<u>Data filtering and resulting network characteristics</u>

Due to limited access to calls among mobile phones and to insufficient information about their spatial location (see PART 1), we included only those mobile phone numbers which had at least one connection to a landline phone. Subsequently, in order to avoid a potential bias induced by multi-user lines and business hubs, we followed the data filtering procedure proposed in (*5*). Hence, we considered only the REC network, and we further excluded all nodes with a degree larger than 50, as well as all links with a call volume exceeding the maximum value observed for those links involving mobile phone users. The summary statistics of the resulting communication network are given in Table S3.

Network type	n^{tot}	m^{tot}	n^{land}	$\langle k^{\text{land}} \rangle$	$\langle v^{\text{land}} \rangle$ [hours]	$\langle \omega^{\text{land}} \rangle$	LCC
REC	47,072,81	119,725,827	24,054,94	7.97	6.61	102.1	0.99

Table S3. Summary statistics of the UK communication network. The number of nodes (n^{tot}) and number of links (m^{tot}) correspond to the LCC of the overall network (including mobile phones connected to landlines). All other values correspond to the landlines only.

Assigning nodes to urban agglomerations

We assigned an exchange area together with its set of landline numbers to an UAC, if the center point of the former is located within the polygon of the latter. This results in 24 UAC containing at least one exchange area. Table S4 shows the corresponding population characteristics. Figure S2 depicts the city size distribution and the number of assigned landline numbers relative to the resident population.

Agglomeration type	No. of entities	N^{tot}	N^{min}	N^{max}
Urban Audit Cities	24	14,186,179	79,734	7,172,091

Table S4. Population statistics of the analyzed urban system for the year 2001. The variables are defined as in Table S2.
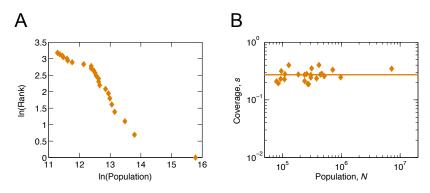

Fig. S2. City size distribution and relative number of landline phones. **(A)** Zipf (rank-size) plot for the population of the Urban Audit Cities. **(B)** Corresponding landline phone coverage. The solid line corresponds to the average value.

PART 3. INDIVIDUAL-BASED INTERACTION DISTRIBUTIONS

I. Selecting a homogeneous set of callers

The individual-based interaction measures derived from mobile phone data in Portugal (degree k, call volume v and number of calls ω) are inherently time-aggregated values. For instance, the degree represents the accumulated number of an individual's contacts, as far as they appear within the overall observation window ΔT. It is therefore evident that these measures become highly affected by longer periods of call inactivity due to, e.g., holidays or cancelling an ongoing (or starting a new) subscription

7

during ΔT. Those callers that are not active on a regular basis naturally induce a bias resulting in negative (left) skewness in the distributions of k, v and ω, as their accumulated measures remain at lower values (Fig. S3).
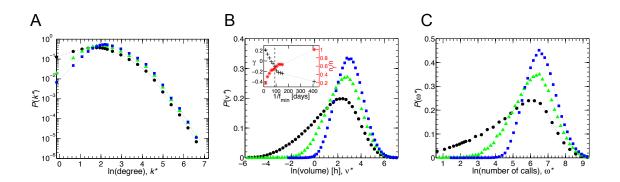

Fig. S3. Removing infrequent callers increases the homogeneity of the interaction distributions. **(A)** Degree distribution for the overall reciprocal mobile phone network in Portugal (REC, ΔT =409 days). To highlight the tail behavior of $k^* = \ln k$, we show the probabilities on a logarithmic scale. **(B and C)** corresponding distribution of the call volume and number of calls, respectively. When considering all callers (black circles) the distributions are strongly left-skewed. Considering only callers whose call frequency is higher than $f_{\min}$ =1/[90 days] (green triangles) and $f_{\min}$ =1/[30 days] (blue squares) gradually decreases the skewness. Most notably for $v^* = \ln v$ and $\omega^* = \ln \omega$, the resulting distributions of the homogenized data increasingly resemble the Gaussian bell curve (i.e., a lognormal distribution in the original variables). The dotted lines serve as a guide to the eye. The inset in **(B)** depicts the decrease of the average skewness, γ, for all Statistical Cities with increasing minimum activity frequency, together with the corresponding fraction of regularly active callers, n_f / n. Note that the fraction of regularly active callers rapidly decreases when $f_{\min}$ >1/[90 days] (dashed line).

Hence, in order to reduce this bias and to compare the individual-based call activity distributions in a meaningful way (*6*), we focus the detailed statistical analysis on regularly active callers. Therefore, while considering the entire reciprocal network (see

8

Table S1), we calculated the probability distributions based on those individuals that initiate and receive at least one call every f_{min} subsequent days. Less active individuals are included in terms of their connections to those 'regularly active' callers. Indeed, as shown in more detail for the example of the call volume (Fig. S3B, inset), increasing the minimum call activity frequency f_{min} effectively decreases the negative skewness of the distributions, which can be quantified by the third standardized moment as

$$\gamma = \frac{E\left\{\left(Y - E\{Y\}\right)^3\right\}}{\text{var}\{Y\}^{3/2}}, \tag{S1}$$

where Y denotes the natural logarithm of a given interaction indicator. Most notably for $v^* = \ln v$ and $\omega^* = \ln \omega$, the distributions increasingly resemble the Gaussian bell curve with increasing f_{min} (very large values of f_{min} even induce a slightly positive skewness). We chose $f_{min} = 1/[90 \text{ days}]$ which substantially decreases the negative skewness (see Fig. S3B, inset), while considering over 50% of all nodes in the reciprocal network (i.e., $n_f = 8.7 \times 10^5$ nodes) as regularly active. Lower values of f_{min} imply highly skewed distributions, while higher values of f_{min} involve a substantially lower fraction of nodes. Despite these changes in the shape of the distributions, the superlinear scaling of the mean is not affected by the value of f_{min}.

In addition to choosing a minimum activity frequency, we tested alternative methods of homogenizing the set of callers. For instance, we selected only individuals that appeared both in the first and last month of the overall observation period, yielding again qualitatively similar results to those reported in the main text. In all cases, the mean of the distributions showed superlinear scaling compatible with the results of Table 1 in the main text.

II. Probability distributions

We applied formal statistical techniques in order to choose the probability model that best describes the homogenized distributions of the degree k, the call volume v and the number of calls ω in the mobile phone interaction network. Given the fat tail of these empirical distributions (Fig. S3) and following an extensive review of related literature,

we selected as trial models (i) the lognormal distribution, (ii) the generalized Pareto distribution, (iii) the double Pareto-lognormal distribution and (iv) the log-skew-normal distribution (also termed 'skewed lognormal distribution').

The lognormal distribution (LN) of a random variable X implies that its logarithm $Y = \ln X$ is normally distributed with probability density

$$P(y) = \frac{1}{\sigma} \phi \left(\frac{y - \mu}{\sigma} \right) \tag{S2}$$

where ϕ denotes the density function of the standard normal distribution, and μ and σ are the mean and standard deviation, respectively. Lognormal distributions are naturally generated by multiplicative random processes and thus are widespread in sociology and economics (*7*).

The density function of the generalized Pareto distribution (GP) with shape parameter α and scale parameter $\sigma > 0$ is given as

$$P(x) = \frac{1}{\sigma} \left(1 + \frac{\alpha}{\sigma} x \right)^{-1/\alpha - 1} \tag{S3}$$

for $x > 0$ if $\alpha \geq 0$ (or for $0 < x < \sigma / |\alpha|$ if $\alpha < 0$) (*8*). The generalized Pareto distribution includes both the exponential and the Pareto distribution as special cases. The latter is a specific and commonly used power law distribution. During the last decade, power laws have attracted much attention in the study of large-scale social networks (*9*), where their appearance has often been attributed to the well-known 'rich gets richer' effect (*7*). In particular, the power law model has been used to describe the degree distribution in mobile phone networks (*10*). Furthermore, a power law degree distribution at the national level can result from lognormal distributions at the city level, when integrated over the city size distribution (Zipf's law), see (*11*).

The double Pareto-lognormal distribution (DPLN) of X implies that $Y = \ln X$ follows a normal-Laplace distribution with probability density

$$P(y) = \frac{\alpha\lambda}{\alpha + \lambda} \phi\left(\frac{y-\theta}{\tau}\right) \left[R\big(\alpha\tau - (y-\theta)/\tau\big) + R\big(\lambda\tau + (y-\theta)/\tau\big) \right] \tag{S4}$$

where $R(z) = \Phi^c(z)/\phi(z)$, with Φ^c being the complementary cumulative distribution function of a standard normal distribution (*12*). While the DPLN has a total of four parameters ($\alpha, \lambda, \theta, \tau$) and thus involves a higher fitting complexity, it has recently been shown to accurately model the empirical distributions of the degree, call volume and number of calls in a mobile phone network (*13*). Similar to the elementary lognormal distribution, the DPLN can be derived from an underlying multiplicative process (*7*).

Finally, a random variable X follows a log-skew-normal distribution (LSN) (*14*) if its logarithm $Y = \ln X$ obeys a skew-normal distribution with density function

$$P(y) = \frac{2}{\theta} \phi\left(\frac{y-\xi}{\theta}\right) \Phi\left(\alpha\left(\frac{y-\xi}{\theta}\right)\right), \tag{S5}$$

where ξ, θ and α are the location, scale and shape parameters, respectively. By allowing for non-zero skewness, Eq. S5 constitutes a generalization of the normal distribution (corresponding to $\alpha = 0$). To simplify the interpretation and to increase the tractability, the 'direct parameters' (ξ, θ, α) can be transformed into the 'centred parameters' (μ, σ, γ) where $\mu = E\{Y\}$, $\sigma^2 = \text{var}\{Y\}$ and γ denotes the skewness of the distribution (Eq. S1). Technical details about the transformation are given in (*15*).

III. Model selection

To compare the different probability distributions for the homogeneous set of callers ($f_{\min} = 1/[90 \text{ days}]$, see section I), we first calculated for each interaction indicator, each model i and individual city c the maximum value of the log-likelihood function, $\ln L_{i,c}$ (see, e.g., (*16*) for an introduction to the maximum likelihood method), and subsequently deployed it to quantify the Bayesian information criterion (BIC) as

$$\mathrm{BIC}_{i,c} = -2\ln L_{i,c} + \eta_i \ln |S_c|, \tag{S6}$$

where η_i is the number of parameters used in model i and $|S_c|$ is the sample size (number of callers assigned to city c). The model with the lowest BIC is selected as the best model. For the three interaction indicators degree, call volume and number of calls (REC network, $\Delta T = 409$ days, $f_{\min} = 1/[90 \text{ days}]$), Tables S5, S6 and S7 indicate how many times each distribution has outperformed all other models in terms of the log-likelihood function and the BIC. The two Larger Urban Zones located on the archipelagos (Ponta Delgada and Funchal) are not considered due to a substantially lower market share ($s < 0.01$ for the homogeneous set of callers). For the call volume, we further discarded 1 Statistical City to which only 4 regularly active callers were assigned (implying s.e.m > 0.9). The log-skew-normal distribution is in most cases the best model for the degree distribution (Table S5). In particular, Eq. S5 provides an excellent fit for the right tail of the distribution which is clearly underestimated by the lognormal distribution and overestimated by the DPLN, as illustrated in Fig. S4 for the REC network. Regarding the call volume and number of calls, the BIC favors the lognormal distribution for both indicators, mainly due to the minimum number of parameters.

Agglomeration type	No. of entities	Statistical method	Distribution model			
			LN	GP	DPLN	LSN
Statistical Cities	140	$\ln L$	0	0	52	88
		BIC	50	1	20	69
Larger Urban Zones	7	$\ln L$	0	0	5	2
		BIC	0	0	3	4
Municipalities	293	$\ln L$	1	1	116	175
		BIC	142	5	15	131
All types	440	$\ln L$	1	1	173	265
		BIC	192	6	38	204

Table S5. Model selection for the degree distribution by the 'goodness of the fit' (REC network, $\Delta T = 409$ days, $f_{\min} = 1/[90 \text{ days}]$). The numbers indicate how many times each distribution has been selected based on the maximum value of the log-likelihood function ($\ln L$) and the BIC, respectively.

Agglomeration type	No. of entities	Statistical method	Distribution model			
			LN	GP	DPLN	LSN
Statistical Cities	139	ln L	0	0	32	107
		BIC	91	7	6	35
Larger Urban Zones	7	ln L	0	0	1	6
		BIC	2	0	0	5
Municipalities	293	ln L	0	0	86	207
		BIC	225	13	3	52
All types	439	ln L	0	0	119	320
		BIC	318	20	9	92

Table S6. Model selection for the distribution of the call volume.

Agglomeration type	No. of entities	Statistical method	Distribution model			
			LN	GP	DPLN	LSN
Statistical Cities	140	ln L	0	0	29	111
		BIC	53	4	8	75
Larger Urban Zones	7	ln L	0	0	0	7
		BIC	0	0	0	7
Municipalities	293	ln L	0	2	89	202
		BIC	170	13	6	104
All types	440	ln L	0	2	118	320
		BIC	223	17	14	186

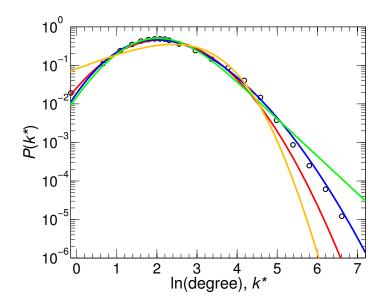**Table S7.** Model selection for the distribution of the number of calls.

13

Fig. S4. Best-fit probability distributions for the degree. Degree distribution (black circles) of the regularly active callers ($f_{min} = 1/[90 \text{ days}]$) in Portugal (REC, $\Delta T = 409$ days). The continuous lines are best fits of the lognormal (red), generalized Pareto (yellow), double Pareto-lognormal (green) and log-skew-normal model (blue).

Interestingly, with increasing homogeneity of the callers with respect to their activity period (i.e., increasing f_{min}, see section I), the lognormal distribution increasingly outperforms the other models. Taking the call volume as an example, the BIC selects the lognormal distribution for only 11 cities when all callers are included (corresponding to $f_{min} = 1/[409 \text{ days}]$). For $f_{min} = 1/[90 \text{ days}]$, the LN is the preferred model in already 96 cases, and for $f_{min} = 1/[60 \text{ days}]$ the LN yields the lowest BIC for 124 cities. This increasing superiority with increasing data homogeneity further supports the lognormal distribution as an appropriate model for the individual-based interaction statistics (call volume and number of calls).

IV. Right-skewness of $P(k^*)$

While the empirical distributions of the logarithms of the call volume, $P(v^*)$, and number of calls, $P(\omega^*)$, are well described by the conventional lognormal distribution,

14

there remains a slight yet non-negligible right-skewness in the distribution of the logarithm of the degree, $P(k^*)$, even when considering only regularly active callers (see section III). Generally, right-skewness can be explained by a 'hidden' constraint on small values (or lower truncation) of otherwise normally distributed observations (see, e.g., (17) for technical details). From this perspective, the right-skewness in $P(k^*)$ can be interpreted as the result of a minimum number of (log-normally distributed) contacts each individual maintains to become observable in the telecommunication data. As each single contact may involve several phone calls with different durations, this lower truncation effect becomes less apparent in $P(v^*)$ and $P(\omega^*)$. Generally, however, the mechanism that introduces constraints or selection is not directly available and must be inferred. We intend to elaborate on this point in future work.

PART 4. MODEL OF NETWORK GROWTH WITH CONSTANT CLUSTERING COEFFICIENT

We have observed that the total connectivity of the phone networks scales superlinearly with urban population

$$K = K_0 N^\beta, \tag{S7}$$

where $\beta \approx 1.12 > 1$ and K_0 is a normalization constant. Consequently, if we assume that this relation holds for full coverage ($s = 1$ so that $|S| = N$), then the connectivity per capita increases, on average, as

$$\langle k \rangle = K_0 N^\delta, \tag{S8}$$

with $\delta = \beta - 1$. Thus, when the network increases in size by one unit, $N \to N + 1$, we obtain a corresponding increase in connectivity,

$$\Delta K = (1 + \delta)\frac{K}{N} = (1 + \delta)\langle k \rangle, \tag{S9}$$

15

which is the number of connections introduced because of the new individual, as she joins the city. How is this average increase in connectivity compatible with a constant clustering coefficient? To answer this question, we construct a model of network growth that shows how the total increase in connectivity, consistent with scaling, is distributed in the network, while satisfying the condition of constant clustering. The key insight is that the invariance of the clustering coefficient requires that the addition of a node also changes the links between its neighbours. In turn, this propagates to their neighbours and so on, leading to a 'cascade' across the network. The magnitude of these effects - number of new links - as a function of distance to the new node is controlled by powers of the average clustering coefficient, $\langle C \rangle$.

We begin with the addition of a new node with degree k_0 to a network with N nodes. This adds at least k_0 connections, plus those links that are necessary to maintain the clustering coefficient constant. Consider then the k_0 neighbours of the new node:

- Each 'average' neighbour gets an additional connection: $k_1 \rightarrow k_1 + 1$.
- Its clustering coefficient changes to be

$$C_1 = \frac{2\left(e_{ij}^{\text{old}} + e_{ij}^{\text{new node}} + e_{ij}^{\text{others}}\right)}{k_1\left(k_1 + 1\right)} = c, \tag{S10}$$

where e_{ij}^{old} is the number of links between its neighbours that existed prior to the introduction of the new node and that we assume persist thereafter; $e_{ij}^{\text{new node}}$ are the number of links between its neighbours introduced by the new node; and e_{ij}^{others} are new links between other neighbours, not involving the new node. This allows us to compute the total number of new links that involve neighbours of the new node. More specifically,

$$2\left(e_{ij}^{\text{old}} + e_{ij}^{\text{new node}} + e_{ij}^{\text{others}}\right) = ck_1\left(k_1 + 1\right) = ck_1\left(k_1 - 1\right) + 2ck_1 \tag{S11}$$

$$\rightarrow e_{ij}^{\text{others}} = ck_1 - e_{ij}^{\text{new node}} = ck_1\left(1 - \frac{k_0 - 1}{2k_1}\right) \tag{S12}$$

If in the last expression $k_0 = k_1 \gg 1$ we obtain $e_{ij}^{\text{others}} = ck_1/2$, or $c/2$ per node. To reach this last result we had to compute how many new triangles are created by the new node among its neighbours, by assuming the value of its clustering coefficient to be c. This, on average, implies

$$e_{ij}^{\text{new node}} = \frac{c}{2}k_0(k_0 - 1)/k_0 = \frac{c}{2}(k_0 - 1). \tag{S13}$$

It is the subtraction of these triangles that brings the naive effect created by the new node of c connections to $c/2$, provided that the degree of the different nodes is similar.

- Finally, we can now assess how many new links are introduced that involve second order (two hops away) neighbours of our index node and so on. We obtain similar result that $e_{ij}^{\text{others}} = c\Delta k_1(2k_1 - 1) - e_{ij}^{\text{new node}}$. However, the new node is now too far to create triangles so that $e_{ij}^{\text{new node}} = 0$. Thus we obtain $e_{ij}^{\text{others}} = c^2(k_1 - 1/2)$. At the next order it can be shown that the number of links is $c\Delta k_2(k_2 - 1/2) \simeq 2k_2 c^3$, and so on. The result is a series, expressing the number of new links introduced as a function of distance to the new node (hops). If at each distance, including the new node, we can assume that $k_i = \langle k \rangle$, then

$$\langle k \rangle\left(1 + \frac{c}{2} + c^2 + 2c^3 + ...\right) = \langle k \rangle\left(1 + \frac{c}{2}\sum_i (2c)^i\right) = \langle k \rangle\left(1 + \frac{c}{2}\frac{1}{1 - 2c}\right). \tag{S14}$$

We see as the leading effect that the new node introduces $\langle k \rangle(1 + c/2)$ new links into the network. Comparing with the average expectation that follows from the scaling law (Eq. (S9)), we would then identify $\delta = c/2$, which is in excellent agreement with the data as $\beta - 1 = \delta \approx 0.12$ and $\langle C \rangle \approx 0.25$. Higher order terms contribute but the

sum may not be taken to infinity because most social networks have relatively short diameters (*18*). Nevertheless, summing the series in Eq. S14 to infinity gives an upper bound on the scaling exponent of $\delta = c / \left[2(1-2c) \right] \simeq 0.25$.

Thus, we conclude that $\delta \simeq c/2 < c$, which confirms our empirical finding of the constant clustering coefficient. In fact, this theoretical result enforces the condition that the effect of each new node propagates throughout the network and that this change of the number of links should be at the heart of the superlinear effects in socioeconomic urban indicators. In the more complicated case where $k_0 \neq \langle k \rangle$ different numerical values of the clustering coefficient are necessary to match the links introduced on average by the superlinear scaling relation.

References

1. Statistics Portugal, *2001 Census* (http://www.ine.pt).

2. Eurostat, *Urban Audit* (http://www.urbanaudit.org).

3. Autoridade Nacional de Comunicacoes, *Historical Data of Mobile Services* (http://www.anacom.pt).

4. J.-P. Onnela, S. Arbesman, M. C. González, A.-L. Barabási, N. A. Christakis, Geographic constraints on social network groups. *Plos One* **6**, e16939 (2011).

5. N. Eagle, M. Macy, R. Claxton, Network diversity and economic development. *Science* **328**, 1029-1031 (2010).

6. G. Krings, M. Karsai, S. Bernhardsson, V. D. Blondel, J. Saramäki, Effects of time window size and placement on the structure of aggregated networks. *EPJ Data Sci.* **1**, 1-16 (2012).

7. M. Mitzenmacher, A brief history of generative models for power law and lognormal distributions. *Internet Math.* **1**, 226-251 (2004).

8. J. Hüsler, D. Li, M. Raschke, Estimation for the generalized Pareto distribution using maximum likelihood and goodness of fit. *Commun Stat. - Theor. M.* **40**, 2500-2510 (2011).

9. A. Clauset, C. R. Shalizi, M. E. J. Newman, Power-law distributions in empirical data. *SIAM Rev.* **51**, 661-703 (2009).

10. J.-P. Onnela, et al. Structure and tie strength in mobile communication networks. *Proc. Natl. Acad. Sci. U.S.A.* **104**, 7332-7336 (2007).

11. A. Gomez-Lievano, H. Youn, L. M. A., Bettencourt, The statistics of urban scaling and their connection to Zipf's law. *PLoS ONE* **7**, e40393 (2012).

12. W. Reed, M. Jorgensen, The double pareto-lognormal distribution - a new parametric model for size distribution. *Commun Stat. - Theor. M.* **33**,1733-1753 (2004).

13. M. Seshadri et al. Mobile call graphs: beyond power-law and lognormal distributions. *In Proc. of ACM SIGKDD* (2008).

14. A. Azzalini, A. Capitano, *S*tatistical applications of the multivariate skew-normal distribution. *J. R. Statist. Soc. B* **61**, 579-602 (1999).

15. R. B. Arellano-Valle, A. Azzalini, The centred parametrization for the multivariate skew-normal distribution. *J. Multivariate Anal.* **99**, 1362-1382 (2008).

16. A. C. Davidson, *Statistical Models*. (Cambridge Univ. Press, Cambridge, 2003).

17. A. Azzalini, The skew-normal distribution and related multivariate families. *Scand. J. Statist.* **32**, 159-188 (2005).

18. S. Boccaletti, V. Latora, Y. Moreno, M. Chavez, D. Hwang, Complex networks: structure and dynamics. *Phys. Rep.* **424**, 175-308 (2006).